

Search for Excited and Exotic Muons in the $\mu\gamma$ Decay Channel in $p\bar{p}$ Collisions at $\sqrt{s} = 1.96$ TeV

A. Abulencia,²³ D. Acosta,¹⁷ J. Adelman,¹³ T. Affolder,¹⁰ T. Akimoto,⁵⁵ M. G. Albrow,¹⁶ D. Ambrose,¹⁶ S. Amerio,⁴³ D. Amidei,³⁴ A. Anastassov,⁵² K. Anikeev,¹⁶ A. Annovi,¹⁸ J. Antos,¹ M. Aoki,⁵⁵ G. Apollinari,¹⁶ J.-F. Arguin,³³ T. Arisawa,⁵⁷ A. Artikov,¹⁴ W. Ashmanskas,¹⁶ A. Attal,⁸ F. Azfar,⁴² P. Azzi-Bacchetta,⁴³ P. Azzurri,⁴⁶ N. Bacchetta,⁴³ H. Bachacou,²⁸ W. Badgett,¹⁶ A. Barbaro-Galtieri,²⁸ V. E. Barnes,⁴⁸ B. A. Barnett,²⁴ S. Baroiant,⁷ V. Bartsch,³⁰ G. Bauer,³² F. Bedeschi,⁴⁶ S. Behari,²⁴ S. Belforte,⁵⁴ G. Bellettini,⁴⁶ J. Bellinger,⁵⁹ A. Belloni,³² E. Ben Haim,⁴⁴ D. Benjamin,¹⁵ A. Beretvas,¹⁶ J. Beringer,²⁸ T. Berry,²⁹ A. Bhatti,⁵⁰ M. Binkley,¹⁶ D. Bisello,⁴³ R. E. Blair,² C. Blocker,⁶ B. Blumenfeld,²⁴ A. Bocci,¹⁵ A. Bodek,⁴⁹ V. Boisvert,⁴⁹ G. Bolla,⁴⁸ A. Bolshov,³² D. Bortoletto,⁴⁸ J. Boudreau,⁴⁷ A. Boveia,¹⁰ B. Brau,¹⁰ C. Bromberg,³⁵ E. Brubaker,¹³ J. Budagov,¹⁴ H. S. Budd,⁴⁹ S. Budd,²³ K. Burkett,¹⁶ G. Busetto,⁴³ P. Bussey,²⁰ K. L. Byrum,² S. Cabrera,¹⁵ M. Campanelli,¹⁹ M. Campbell,³⁴ F. Canelli,⁸ A. Canepa,⁴⁸ D. Carlsmith,⁵⁹ R. Carosi,⁴⁶ S. Carron,¹⁵ B. Casal,¹¹ M. Casarsa,⁵⁴ A. Castro,⁵ P. Catastini,⁴⁶ D. Cauz,⁵⁴ M. Cavalli-Sforza,³ A. Cerri,²⁸ L. Cerrito,⁴² S. H. Chang,²⁷ J. Chapman,³⁴ Y. C. Chen,¹ M. Chertok,⁷ G. Chiarelli,⁴⁶ G. Chlachidze,¹⁴ F. Chlebana,¹⁶ I. Cho,²⁷ K. Cho,²⁷ D. Chokheli,¹⁴ J. P. Chou,²¹ P. H. Chu,²³ S. H. Chuang,⁵⁹ K. Chung,¹² W. H. Chung,⁵⁹ Y. S. Chung,⁴⁹ M. Ciljak,⁴⁶ C. I. Ciobanu,²³ M. A. Ciocci,⁴⁶ A. Clark,¹⁹ D. Clark,⁶ M. Coca,¹⁵ G. Compostella,⁴³ M. E. Convery,⁵⁰ J. Conway,⁷ B. Cooper,³⁰ K. Copic,³⁴ M. Cordelli,¹⁸ G. Cortiana,⁴³ F. Crescioli,⁴⁶ A. Cruz,¹⁷ C. Cuenca Almenar,⁷ J. Cuevas,¹¹ R. Culbertson,¹⁶ D. Cyr,⁵⁹ S. DaRonco,⁴³ S. D'Auria,²⁰ M. D'Onofrio,³ D. Dagenhart,⁶ P. de Barbaro,⁴⁹ S. De Cecco,⁵¹ A. Deisher,²⁸ G. De Lentdecker,⁴⁹ M. Dell'Orso,⁴⁶ F. Delli Paoli,⁴³ S. Demers,⁴⁹ L. Demortier,⁵⁰ J. Deng,¹⁵ M. Deninno,⁵ D. De Pedis,⁵¹ P. F. Derwent,¹⁶ G. P. Di Giovanni,⁴⁴ B. Di Ruzza,⁵⁴ C. Dionisi,⁵¹ J. R. Dittmann,⁴ P. DiTuro,⁵² C. Dörr,²⁵ S. Donati,⁴⁶ M. Donega,¹⁹ P. Dong,⁸ J. Donini,⁴³ T. Dorigo,⁴³ S. Dube,⁵² K. Ebina,⁵⁷ J. Efron,³⁹ J. Ehlers,¹⁹ R. Erbacher,⁷ D. Errede,²³ S. Errede,²³ R. Eusebi,¹⁶ H. C. Fang,²⁸ S. Farrington,²⁹ I. Fedorko,⁴⁶ W. T. Fedorko,¹³ R. G. Feild,⁶⁰ M. Feindt,²⁵ J. P. Fernandez,³¹ R. Field,¹⁷ G. Flanagan,⁴⁸ L. R. Flores-Castillo,⁴⁷ A. Foland,²¹ S. Forrester,⁷ G. W. Foster,²⁸ M. Franklin,²¹ J. C. Freeman,²⁸ H. J. Frisch,¹³ I. Furic,¹³ M. Gallinaro,⁵⁰ J. Galyardt,¹² J. E. Garcia,⁴⁶ M. Garcia Sciveres,²⁸ A. F. Garfinkel,⁴⁸ C. Gay,⁶⁰ H. Gerberich,²³ D. Gerdes,³⁴ S. Giagu,⁵¹ P. Giannetti,⁴⁶ A. Gibson,²⁸ K. Gibson,¹² C. Ginsburg,¹⁶ N. Giokaris,¹⁴ K. Giolo,⁴⁸ M. Giordani,⁵⁴ P. Giromini,¹⁸ M. Giunta,⁴⁶ G. Giurgiu,¹² V. Glagolev,¹⁴ D. Glenzinski,¹⁶ M. Gold,³⁷ N. Goldschmidt,³⁴ J. Goldstein,⁴² G. Gomez,¹¹ G. Gomez-Ceballos,¹¹ M. Goncharov,⁵³ O. González,³¹ I. Gorelov,³⁷ A. T. Goshaw,¹⁵ Y. Gotra,⁴⁷ K. Goulianos,⁵⁰ A. Gresele,⁴³ M. Griffiths,²⁹ S. Grinstein,²¹ C. Grosso-Pilcher,¹³ R. C. Group,¹⁷ U. Grundler,²³ J. Guimaraes da Costa,²¹ Z. Gunay-Unalan,³⁵ C. Haber,²⁸ S. R. Hahn,¹⁶ K. Hahn,⁴⁵ E. Halkiadakis,⁵² A. Hamilton,³³ B.-Y. Han,⁴⁹ J. Y. Han,⁴⁹ R. Handler,⁵⁹ F. Happacher,¹⁸ K. Hara,⁵⁵ M. Hare,⁵⁶ S. Harper,⁴² R. F. Harr,⁵⁸ R. M. Harris,¹⁶ K. Hatakeyama,⁵⁰ J. Hauser,⁸ C. Hays,¹⁵ A. Heijboer,⁴⁵ B. Heinemann,²⁹ J. Heinrich,⁴⁵ M. Herndon,⁵⁹ D. Hidas,¹⁵ C. S. Hill,¹⁰ D. Hirschbuehl,²⁵ A. Hocker,¹⁶ A. Holloway,²¹ S. Hou,¹ M. Houlden,²⁹ S.-C. Hsu,⁹ B. T. Huffman,⁴² R. E. Hughes,³⁹ J. Huston,³⁵ J. Incandela,¹⁰ G. Introzzi,⁴⁶ M. Iori,⁵¹ Y. Ishizawa,⁵⁵ A. Ivanov,⁷ B. Iyutin,³² E. James,¹⁶ D. Jang,⁵² B. Jayatilaka,³⁴ D. Jeans,⁵¹ H. Jensen,¹⁶ E. J. Jeon,²⁷ S. Jindariani,¹⁷ M. Jones,⁴⁸ K. K. Joo,²⁷ S. Y. Jun,¹² T. R. Junk,²³ T. Kamon,⁵³ J. Kang,³⁴ P. E. Karchin,⁵⁸ Y. Kato,⁴¹ Y. Kemp,²⁵ R. Kephart,¹⁶ U. Kerzel,²⁵ V. Khotilovich,⁵³ B. Kilminster,³⁹ D. H. Kim,²⁷ H. S. Kim,²⁷ J. E. Kim,¹⁵ M. J. Kim,¹² S. B. Kim,²⁷ S. H. Kim,⁵⁵ Y. K. Kim,¹³ L. Kirsch,⁶ S. Klimentenko,¹⁷ M. Klute,³² B. Knuteson,³² B. R. Ko,¹⁵ H. Kobayashi,⁵⁵ K. Kondo,⁵⁷ D. J. Kong,²⁷ J. Konigsberg,¹⁷ A. Korytov,¹⁷ A. V. Kotwal,¹⁵ A. Kovalev,⁴⁵ A. Kraan,⁴⁵ J. Kraus,²³ I. Kravchenko,³² M. Kreps,²⁵ J. Kroll,⁴⁵ N. Krumnack,⁴ M. Kruse,¹⁵ V. Krutelyov,⁵³ S. E. Kuhlmann,² Y. Kusakabe,⁵⁷ S. Kwang,¹³ A. T. Laasanen,⁴⁸ S. Lai,³³ S. Lami,⁴⁶ S. Lammel,¹⁶ M. Lancaster,³⁰ R. L. Lander,⁷ K. Lannon,³⁹ A. Lath,⁵² G. Latino,⁴⁶ I. Lazzizzera,⁴³ T. LeCompte,² J. Lee,⁴⁹ J. Lee,²⁷ Y. J. Lee,²⁷ S. W. Lee,⁵³ R. Lefèvre,³ N. Leonardo,³² S. Leone,⁴⁶ S. Levy,¹³ J. D. Lewis,¹⁶ C. Lin,⁶⁰ C. S. Lin,¹⁶ M. Lindgren,¹⁶ E. Lipeles,⁹ T. M. Liss,²³ A. Lister,¹⁹ D. O. Litvintsev,¹⁶ T. Liu,¹⁶ N. S. Lockyer,⁴⁵ A. Loginov,³⁶ M. Loreti,⁴³ P. Loverre,⁵¹ R.-S. Lu,¹ D. Lucchesi,⁴³ P. Lujan,²⁸ P. Lukens,¹⁶ G. Lungu,¹⁷ L. Lyons,⁴² J. Lys,²⁸ R. Lysak,¹ E. Lytken,⁴⁸ P. Mack,²⁵ D. MacQueen,³³ R. Madrak,¹⁶ K. Maeshima,¹⁶ T. Maki,²² P. Maksimovic,²⁴ S. Malde,⁴² G. Manca,²⁹ F. Margaroli,⁵ R. Marginean,¹⁶ C. Marino,²³ A. Martin,⁶⁰ V. Martin,³⁸ M. Martínez,³ T. Maruyama,⁵⁵ P. Mastrandrea,⁵¹ H. Matsunaga,⁵⁵ M. E. Mattson,⁵⁸ R. Mazini,³³ P. Mazzanti,⁵ K. S. McFarland,⁴⁹ P. McIntyre,⁵³ R. McNulty,²⁹ A. Mehta,²⁹ S. Menzemer,¹¹ A. Menzione,⁴⁶ P. Merkel,⁴⁸ C. Mesropian,⁵⁰ A. Messina,⁵¹ M. von der Mey,⁸ T. Miao,¹⁶ N. Miladinovic,⁶ J. Miles,³² R. Miller,³⁵ J. S. Miller,³⁴ C. Mills,¹⁰ M. Milnik,²⁵ R. Miquel,²⁸ A. Mitra,¹ G. Mitselmakher,¹⁷ A. Miyamoto,²⁶ N. Moggi,⁵ B. Mohr,⁸ R. Moore,¹⁶ M. Morello,⁴⁶ P. Movilla Fernandez,²⁸ J. Mülmenstädt,²⁸ A. Mukherjee,¹⁶ Th. Muller,²⁵ R. Mumford,²⁴ P. Murat,¹⁶ J. Nachtman,¹⁶ J. Naganoma,⁵⁷ S. Nahn,³² I. Nakano,⁴⁰ A. Napier,⁵⁶ D. Naumov,³⁷ V. Necula,¹⁷ C. Neu,⁴⁵ M. S. Neubauer,⁹

J. Nielsen,²⁸ T. Nigmanov,⁴⁷ L. Nodulman,² O. Norriella,³ E. Nurse,³⁰ T. Ogawa,⁵⁷ S. H. Oh,¹⁵ Y. D. Oh,²⁷ T. Okusawa,⁴¹ R. Oldeman,²⁹ R. Orava,²² K. Osterberg,²² C. Pagliarone,⁴⁶ E. Palencia,¹¹ R. Paoletti,⁴⁶ V. Papadimitriou,¹⁶ A. A. Paramonov,¹³ B. Parks,³⁹ S. Pashapour,³³ J. Patrick,¹⁶ G. Pauletta,⁵⁴ M. Paulini,¹² C. Paus,³² D. E. Pellett,⁷ A. Penzo,⁵⁴ T. J. Phillips,¹⁵ G. Piacentino,⁴⁶ J. Piedra,⁴⁴ L. Pinera,¹⁷ K. Pitts,²³ C. Plager,⁸ L. Pondrom,⁵⁹ X. Portell,³ O. Poukhov,¹⁴ N. Pounder,⁴² F. Prakoshyn,¹⁴ A. Pronko,¹⁶ J. Proudfoot,² F. Ptohos,¹⁸ G. Punzi,⁴⁶ J. Pursley,²⁴ J. Rademacker,⁴² A. Rahaman,⁴⁷ A. Rakinin,³² S. Rappoccio,²¹ F. Ratnikov,⁵² B. Reiser,¹⁶ V. Rekovic,³⁷ N. van Remortel,²² P. Renton,⁴² M. Rescigno,⁵¹ S. Richter,²⁵ F. Rimondi,⁵ L. Ristori,⁴⁶ W. J. Robertson,¹⁵ A. Robson,²⁰ T. Rodrigo,¹¹ E. Rogers,²³ S. Rolli,⁵⁶ R. Roser,¹⁶ M. Rossi,⁵⁴ R. Rossin,¹⁷ C. Rott,⁴⁸ A. Ruiz,¹¹ J. Russ,¹² V. Rusu,¹³ H. Saarikko,²² S. Sabik,³³ A. Safonov,⁵³ W. K. Sakumoto,⁴⁹ G. Salamanna,⁵¹ O. Saltó,³ D. Saltzberg,⁸ C. Sanchez,³ L. Santi,⁵⁴ S. Sarkar,⁵¹ L. Sartori,⁴⁶ K. Sato,⁵⁵ P. Savard,³³ A. Savoy-Navarro,⁴⁴ T. Scheidle,²⁵ P. Schlabach,¹⁶ E. E. Schmidt,¹⁶ M. P. Schmidt,⁶⁰ M. Schmitt,³⁸ T. Schwarz,³⁴ L. Scodellaro,¹¹ A. L. Scott,¹⁰ A. Scribano,⁴⁶ F. Scuri,⁴⁶ A. Sedov,⁴⁸ S. Seidel,³⁷ Y. Seiya,⁴¹ A. Semenov,¹⁴ L. Sexton-Kennedy,¹⁶ I. Sfiligoi,¹⁸ M. D. Shapiro,²⁸ T. Shears,²⁹ P. F. Shepard,⁴⁷ D. Sherman,²¹ M. Shimojima,⁵⁵ M. Shochet,¹³ Y. Shon,⁵⁹ I. Shreyber,³⁶ A. Sidoti,⁴⁴ P. Sinervo,³³ A. Sisakyan,¹⁴ J. Sjolín,⁴² A. Skiba,²⁵ A. J. Slaughter,¹⁶ K. Sliwa,⁵⁶ J. R. Smith,⁷ F. D. Snider,¹⁶ R. Snihur,³³ M. Soderberg,³⁴ A. Soha,⁷ S. Somalwar,⁵² V. Sorin,³⁵ J. Spalding,¹⁶ M. Spezziga,¹⁶ F. Spinella,⁴⁶ T. Spreitzer,³³ P. Squillacioti,⁴⁶ M. Stanitzki,⁶⁰ A. Staveris-Polykalas,⁴⁶ R. St. Denis,²⁰ B. Stelzer,⁸ O. Stelzer-Chilton,⁴² D. Stentz,³⁸ J. Strologas,³⁷ D. Stuart,¹⁰ J. S. Suh,²⁷ A. Sukhanov,¹⁷ K. Sumorok,³² H. Sun,⁵⁶ T. Suzuki,⁵⁵ A. Taffard,²³ R. Takashima,⁴⁰ Y. Takeuchi,⁵⁵ K. Takikawa,⁵⁵ M. Tanaka,² R. Tanaka,⁴⁰ N. Tanimoto,⁴⁰ M. Tecchio,³⁴ P. K. Teng,¹ K. Terashi,⁵⁰ S. Tether,³² J. Thom,¹⁶ A. S. Thompson,²⁰ E. Thomson,⁴⁵ P. Tipton,⁴⁹ V. Tiwari,¹² S. Tkaczyk,¹⁶ D. Toback,⁵³ S. Tokar,¹⁴ K. Tollefson,³⁵ T. Tomura,⁵⁵ D. Tonelli,⁴⁶ M. Tönnemann,³⁵ S. Torre,¹⁸ D. Torretta,¹⁶ S. Tourneur,⁴⁴ W. Trischuk,³³ R. Tsuchiya,⁵⁷ S. Tsuno,⁴⁰ N. Turini,⁴⁶ F. Ukegawa,⁵⁵ T. Unverhau,²⁰ S. Uozumi,⁵⁵ D. Usynin,⁴⁵ A. Vaiciulis,⁴⁹ S. Vallecorsa,¹⁹ A. Varganov,³⁴ E. Vataga,³⁷ G. Velev,¹⁶ G. Veramendi,²³ V. Veszpremi,⁴⁸ R. Vidal,¹⁶ I. Vila,¹¹ R. Vilar,¹¹ T. Vine,³⁰ I. Vollrath,³³ I. Volobouev,²⁸ G. Volpi,⁴⁶ F. Würthwein,⁹ P. Wagner,⁵³ R. G. Wagner,² R. L. Wagner,¹⁶ W. Wagner,²⁵ R. Wallny,⁸ T. Walter,²⁵ Z. Wan,⁵² S. M. Wang,¹ A. Warburton,³³ S. Waschke,²⁰ D. Waters,³⁰ W. C. Wester III,¹⁶ B. Whitehouse,⁵⁶ D. Whiteson,⁴⁵ A. B. Wicklund,² E. Wicklund,¹⁶ G. Williams,³³ H. H. Williams,⁴⁵ P. Wilson,¹⁶ B. L. Winer,³⁹ P. Wittich,¹⁶ S. Wolbers,¹⁶ C. Wolfe,¹³ T. Wright,³⁴ X. Wu,¹⁹ S. M. Wynne,²⁹ A. Yagil,¹⁶ K. Yamamoto,⁴¹ J. Yamaoka,⁵² T. Yamashita,⁴⁰ C. Yang,⁶⁰ U. K. Yang,¹³ Y. C. Yang,²⁷ W. M. Yao,²⁸ G. P. Yeh,¹⁶ J. Yoh,¹⁶ K. Yorita,¹³ T. Yoshida,⁴¹ G. B. Yu,⁴⁹ I. Yu,²⁷ S. S. Yu,¹⁶ J. C. Yun,¹⁶ L. Zanello,⁵¹ A. Zanetti,⁵⁴ I. Zaw,²¹ F. Zetti,⁴⁶ X. Zhang,²³ J. Zhou,⁵² and S. Zucchelli⁵

(CDF Collaboration)

¹*Institute of Physics, Academia Sinica, Taipei, Taiwan 11529, Republic of China*²*Argonne National Laboratory, Argonne, Illinois 60439, USA*³*Institut de Física d'Altes Energies, Universitat Autònoma de Barcelona, E-08193, Bellaterra (Barcelona), Spain*⁴*Baylor University, Waco, Texas 76798, USA*⁵*Istituto Nazionale di Fisica Nucleare, University of Bologna, I-40127 Bologna, Italy*⁶*Brandeis University, Waltham, Massachusetts 02254, USA*⁷*University of California, Davis, Davis, California 95616, USA*⁸*University of California, Los Angeles, Los Angeles, California 90024, USA*⁹*University of California, San Diego, La Jolla, California 92093, USA*¹⁰*University of California, Santa Barbara, Santa Barbara, California 93106, USA*¹¹*Instituto de Física de Cantabria, CSIC-University of Cantabria, 39005 Santander, Spain*¹²*Carnegie Mellon University, Pittsburgh, Pennsylvania 15213, USA*¹³*Enrico Fermi Institute, University of Chicago, Chicago, Illinois 60637, USA*¹⁴*Joint Institute for Nuclear Research, RU-141980 Dubna, Russia*¹⁵*Duke University, Durham, North Carolina 27708, USA*¹⁶*Fermi National Accelerator Laboratory, Batavia, Illinois 60510, USA*¹⁷*University of Florida, Gainesville, Florida 32611, USA*¹⁸*Laboratori Nazionali di Frascati, Istituto Nazionale di Fisica Nucleare, I-00044 Frascati, Italy*¹⁹*University of Geneva, CH-1211 Geneva 4, Switzerland*²⁰*Glasgow University, Glasgow G12 8QQ, United Kingdom*²¹*Harvard University, Cambridge, Massachusetts 02138, USA*²²*Division of High Energy Physics, Department of Physics, University of Helsinki and Helsinki Institute of Physics, FIN-00014, Helsinki, Finland*

- ²³University of Illinois, Urbana, Illinois 61801, USA
²⁴The Johns Hopkins University, Baltimore, Maryland 21218, USA
²⁵Institut für Experimentelle Kernphysik, Universität Karlsruhe, 76128 Karlsruhe, Germany
²⁶High Energy Accelerator Research Organization (KEK), Tsukuba, Ibaraki 305, Japan
²⁷Center for High Energy Physics: Kyungpook National University, Taegu 702-701, Korea;
 Seoul National University, Seoul 151-742, Korea;
 and SungKyunKwan University, Suwon 440-746, Korea
²⁸Ernest Orlando Lawrence Berkeley National Laboratory, Berkeley, California 94720, USA
²⁹University of Liverpool, Liverpool L69 7ZE, United Kingdom
³⁰University College London, London WC1E 6BT, United Kingdom
³¹Centro de Investigaciones Energeticas Medioambientales y Tecnologicas, E-28040 Madrid, Spain
³²Massachusetts Institute of Technology, Cambridge, Massachusetts 02139, USA
³³Institute of Particle Physics: McGill University, Montréal, Canada H3A 2T8; and University of Toronto, Toronto, Canada M5S 1A7
³⁴University of Michigan, Ann Arbor, Michigan 48109, USA
³⁵Michigan State University, East Lansing, Michigan 48824, USA
³⁶Institution for Theoretical and Experimental Physics, ITEP, Moscow 117259, Russia
³⁷University of New Mexico, Albuquerque, New Mexico 87131, USA
³⁸Northwestern University, Evanston, Illinois 60208, USA
³⁹The Ohio State University, Columbus, Ohio 43210, USA
⁴⁰Okayama University, Okayama 700-8530, Japan
⁴¹Osaka City University, Osaka 588, Japan
⁴²University of Oxford, Oxford OX1 3RH, United Kingdom
⁴³University of Padova, Istituto Nazionale di Fisica Nucleare, Sezione di Padova-Trento, I-35131 Padova, Italy
⁴⁴LPNHE, Universite Pierre et Marie Curie/IN2P3-CNRS, UMR7585, Paris, F-75252 France
⁴⁵University of Pennsylvania, Philadelphia, Pennsylvania 19104, USA
⁴⁶Istituto Nazionale di Fisica Nucleare Pisa, Universities of Pisa, Siena and Scuola Normale Superiore, I-56127 Pisa, Italy
⁴⁷University of Pittsburgh, Pittsburgh, Pennsylvania 15260, USA
⁴⁸Purdue University, West Lafayette, Indiana 47907, USA
⁴⁹University of Rochester, Rochester, New York 14627, USA
⁵⁰The Rockefeller University, New York, New York 10021, USA
⁵¹Istituto Nazionale di Fisica Nucleare, Sezione di Roma 1, University of Rome “La Sapienza,” I-00185 Roma, Italy
⁵²Rutgers University, Piscataway, New Jersey 08855, USA
⁵³Texas A&M University, College Station, Texas 77843, USA
⁵⁴Istituto Nazionale di Fisica Nucleare, University of Trieste/Udine, Italy
⁵⁵University of Tsukuba, Tsukuba, Ibaraki 305, Japan
⁵⁶Tufts University, Medford, Massachusetts 02155, USA
⁵⁷Waseda University, Tokyo 169, Japan
⁵⁸Wayne State University, Detroit, Michigan 48201, USA
⁵⁹University of Wisconsin, Madison, Wisconsin 53706, USA
⁶⁰Yale University, New Haven, Connecticut 06520, USA
 (Received 19 June 2006; published 9 November 2006)

We search for excited and exotic muon states μ^* using an integrated luminosity of 371 pb^{-1} of $p\bar{p}$ collision data at $\sqrt{s} = 1.96 \text{ TeV}$. We search for associated production of $\mu\mu^*$ followed by the decay $\mu^* \rightarrow \mu\gamma$. We compare the data to model predictions as a function of the mass of the excited muon M_{μ^*} , the compositeness energy scale Λ , and the gauge coupling factor f . No signal above the standard model expectation is observed. We exclude $107 < M_{\mu^*} < 853 \text{ GeV}/c^2$ for $\Lambda = M_{\mu^*}$ in the contact interaction model, and $100 < M_{\mu^*} < 410 \text{ GeV}/c^2$ for $f/\Lambda = 10^{-2} \text{ GeV}^{-1}$ in the gauge-mediated model, both at the 95% confidence level.

DOI: [10.1103/PhysRevLett.97.191802](https://doi.org/10.1103/PhysRevLett.97.191802)

PACS numbers: 12.60.Rc, 13.85.Qk, 14.60.Hi

In the standard model (SM) the quarks and leptons are treated as fundamental particles. Their generational structure and observed mass hierarchy motivate a model of composite quarks and leptons consisting of fewer elementary particles than contained in the SM [1]. In this model, quarks and leptons are the lowest-energy bound states of these hypothetical particles, and additional excited states exist near the compositeness energy scale Λ .

Exotic fermions are also predicted in the context of grand unified or string theories, in which the known forces are unified into a larger symmetry group [2]. In such models, additional fermions are predicted with properties similar to those of excited fermions.

At a $p\bar{p}$ collider, excited or exotic muon states could be observed through the reaction $q\bar{q} \rightarrow \mu^*\mu$. Excited muon production can be described using a contact interaction

(CI) Lagrangian density [1]:

$$L = \frac{4\pi}{\Lambda^2} \bar{q}_L \gamma^\mu q_L \bar{M}_L \gamma_\mu \mu_L + \text{H.c.},$$

where M_L represents the left-handed μ^* field, and right-handed currents have been neglected for simplicity. For exotic muon production, the relevant gauge-mediated (GM) Lagrangian density is [3]:

$$L = \frac{1}{2\Lambda} (\bar{M}_R \bar{N}_R) \sigma^{\mu\nu} \left[f g \frac{\vec{\tau}}{2} \cdot \vec{W}_{\mu\nu} + f' g' \frac{Y}{2} B_{\mu\nu} \right] \begin{pmatrix} \mu_L \\ \nu_L \end{pmatrix} + \text{H.c.},$$

where N_R is the excited neutrino field, W and B are the $SU(2)_L$ and $U(1)_Y$ field strengths, g and g' are the respective electroweak couplings, and f and f' are phenomenological constants which are set equal to each other by convention to maximize the photonic decay branching ratio. For $f = f'$ ($f = -f'$), the relative μ^* branching ratios are $\text{BR}(\mu^* \rightarrow \mu\gamma) \approx 0.3$ (0), $\text{BR}(\mu^* \rightarrow \nu W) \approx 0.6$ (0.6), and $\text{BR}(\mu^* \rightarrow \mu Z) \approx 0.1$ (0.4) for $M_{\mu^*} > 200 \text{ GeV}/c^2$. The $\text{BR}(\mu^* \rightarrow \mu\gamma)$ increases to 70% at $M_{\mu^*} = 100 \text{ GeV}/c^2$ for $f = f'$. We use these branching ratios for both the GM and CI production models [4], and we also quote the CI model result with the branching ratio corrected for CI decays.

In this Letter we describe the first hadron-collider search for associated $\mu\mu^*$ production in the context of the GM model, and extend existing mass limits in both the GM and CI models. Prior searches for μ^* production have been performed by the LEP experiments, which have excluded μ^* with $M_{\mu^*} < 200 \text{ GeV}/c^2$ for $f/\Lambda > 10^{-2} \text{ GeV}^{-1}$ in the GM model [5]. The D0 experiment has excluded μ^* with $M_{\mu^*} < 688 \text{ GeV}/c^2$ for $\Lambda = M_{\mu^*}$ in a particular CI model [6]. The most recent measurement of $(g_\mu - 2)$ [7] sets an indirect lower limit on M_{μ^*} of $\mathcal{O}(400 \text{ GeV}/c^2)$, assuming chiral symmetry of the excited state [8].

We use 371 pb^{-1} of data collected with the CDF II detector [9] at the Fermilab Tevatron. The detector's magnetic spectrometer consists of silicon microstrip and drift-chamber [10] tracking detectors. Surrounding this are central [11] ($|\eta| < 1$ [12]) and forward [13] ($|\eta| > 1.1$) electromagnetic (EM) and hadronic calorimeters. Embedded in the central EM calorimeter are wire and strip chambers [9] (used to measure the transverse shower profiles of photons) and a central preshower detector [9] (used for detecting photon conversions). Outside the calorimeters are CMUP ($|\eta| < 0.6$) and CMX ($0.6 < |\eta| < 1$) muon detectors [14]. The momentum resolution of beam-constrained drift-chamber tracks is $\delta p_T/p_T^2 \approx 0.05\%/(\text{GeV}/c)$. The electromagnetic energy resolution for photons from μ^* decays is $\approx 2.5\%$.

We analyze events passing the trigger requirement of one drift-chamber track with $p_T > 18 \text{ GeV}/c$ [12] matched to a reconstructed track segment in the muon

chambers. In the offline analysis, we require two muon candidates identified by drift-chamber tracks with $p_T > 20 \text{ GeV}/c$ and $|\eta| < 1$, which pass requirements on impact parameter and number of hits, have minimum-ionizing particle properties, and at least one of which has a matching muon chamber segment [15]. Both tracks must pass isolation requirements based on calorimetric and tracking energy flow in their vicinity. Finally, we reject cosmic rays based on tracking and track-timing information [16].

We select dimuon events that have a photon candidate with $E_T > 25 \text{ GeV}$ and $|\eta| < 2.8$. Photons are identified by their longitudinal and transverse calorimeter shower profiles, and by the lack of tracks and calorimeter energy in their vicinity [4]. To suppress the initial-state radiation (ISR) $Z(\rightarrow \mu\mu)\gamma$ background, we reject events with dimuon invariant mass $m_{\mu\mu}$ in the range 81–101 GeV/c^2 .

A $Z \rightarrow \mu\mu$ sample is used to measure the efficiencies of the muon identification criteria and trigger. The efficiency of the calorimeter and tracking identification requirements is measured to be $(92.6 \pm 0.3_{\text{stat}})\%$. We measure the combined trigger and muon chamber matching efficiency to be $(79.3 \pm 1.0_{\text{stat}})\%$ for the CMUP and $(95.0 \pm 0.6_{\text{stat}})\%$ for the CMX.

The photon identification efficiency is extracted from a GEANT-based detector simulation [17]. Since photons and electrons have similar electromagnetic showers, we validate the simulated photon efficiency using a control sample of electrons from $Z \rightarrow ee$ events [4].

The geometric acceptance is calculated with the GEANT detector simulation separately for the CI and GM models. We use the PYTHIA [18] generator for the CI model and the LANHEP [19] and COMPHEP [20] programs to generate GM model events. The two models generate similar kinematic and angular distributions for the final-state particles. The total signal acceptance (including identification efficiencies) for the CI (GM) model increases from 13% (12%) at $M_{\mu^*} = 100 \text{ GeV}/c^2$ to an asymptotic value of 21% (23%) for $M_{\mu^*} > 400$ (300) GeV/c^2 . The relative systematic uncertainty on the acceptance is 3.1%, which is dominated by the uncertainty in the identification efficiency (2.2%) and simulation statistics (2.0%).

We compute the expected background contributions from the following sources: (1) $Z/\gamma^*(+\gamma) \rightarrow \mu\mu\gamma$, (2) $Z/\gamma^*(+\gamma) \rightarrow \tau\tau\gamma$, where the τ 's decay to muons, (3) $Z/\gamma^*(\rightarrow \mu\mu) + \text{jet}$, where the jet is misidentified as a photon, (4) $t(\rightarrow \mu\nu b) + \bar{t}(\rightarrow \mu\nu \bar{b})$, where a fermion radiates a photon, (5) $W(\rightarrow e\nu) + Z(\rightarrow \mu\mu)$, where the electron is misidentified as a photon, and (6) $Z(\rightarrow ee) + Z(\rightarrow \mu\mu)$, where one of the electrons is misidentified as a photon. Other backgrounds (≥ 3 jets, $W + \geq 2$ jets, $W\gamma + \geq 1$ jet, and cosmic rays) were found to be negligible.

The $Z\gamma$, $t\bar{t}$, WZ , and ZZ backgrounds are estimated using simulated events, with the ZGAMMA [21] generator

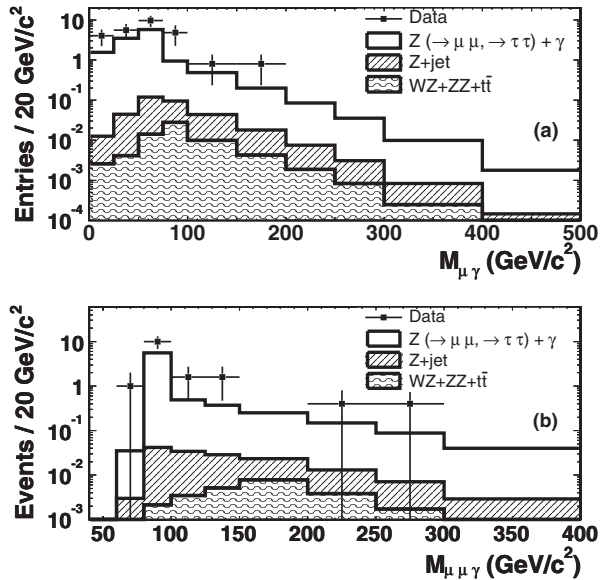


FIG. 1. The $\mu\gamma$ (a) and $\mu\mu\gamma$ (b) mass distributions for the data with background expectations. The total number of observed (expected) $\mu\mu\gamma$ entries is 17 (8.3 ± 0.9). Both $\mu\gamma$ combinations per event are included in (a).

for the $Z(\rightarrow \mu\mu)\gamma$ background and PYTHIA for the others. Systematic uncertainties on these background predictions arise due to integrated luminosity (6%) [22], parton distribution functions (PDFs) (5%), higher-order QCD corrections (5%) [23], acceptance (1%), and identification efficiencies (2%).

The $Z + \text{jet}$ background is estimated by weighting $Z + \text{jet}$ events from the data by an E_T -dependent jet $\rightarrow \gamma$ misidentification rate. The latter is measured using a jet-triggered data sample, correcting for the fraction of true prompt photons in the jet sample [4]. The prompt photon fraction is estimated using $\gamma \rightarrow ee$ conversions identified with the calorimeter preshower detector [24]. The jet $\rightarrow \gamma$ misidentification rate is applied as a function of E_T in the central calorimeter and as a function of E_T and η in the forward calorimeter.

We observe 17 signal candidates with a background prediction of 8.3 ± 0.9 , of which 8.1 ± 0.8 are expected from $Z\gamma$ production. The Poisson probability for the back-

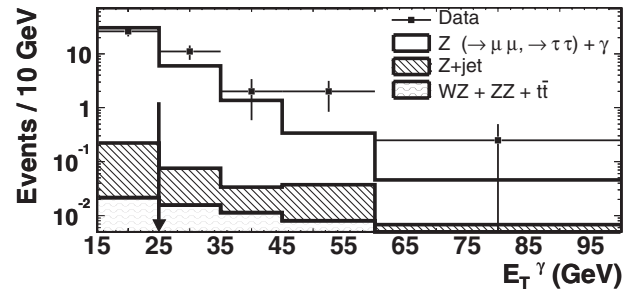


FIG. 2. The E_T^γ distributions for the data (43 events) and background (38.5 ± 4.0 events) expectations for $E_T^\gamma > 15$ GeV. The arrow indicates the minimum E_T^γ required for this analysis.

ground to fluctuate up to the observation, or higher, is 0.8%. Eleven events have a 3-body mass $m_{\mu\mu\gamma}$ in the 81–101 GeV/c^2 range, consistent with being final-state radiation (FSR) $Z \rightarrow \mu\mu\gamma$ events, to be compared to the FSR $Z \rightarrow \mu\mu\gamma$ prediction of 5.5 ± 0.5 events. Figure 1 and Table I show the $m_{\mu\gamma}$ and $m_{\mu\mu\gamma}$ distributions for the data and background.

To test our background prediction, we lower the minimum photon E_T to 15 GeV and observe 43 events with a prediction of 38.5 ± 4.0 events. The data show good agreement with expectation in this higher statistics sample, as shown in Fig. 2. Additionally, we find consistency in the ISR $Z\gamma$ control region of $81 < m_{\mu\mu} < 101$ GeV/c^2 and $25 < E_T^\gamma < 50$ GeV, where we observe 5 events with a prediction of $7.2^{+1.2}_{-0.8}$ events. Finally, we find our candidate sample to be stable under variations of the muon selection criteria. We conclude that our signal sample has an upward statistical fluctuation, dominantly in the number of FSR $Z \rightarrow \mu\mu\gamma$ events.

For the μ^* resonance search, we scan the $m_{\mu\gamma}$ spectrum with a sliding window of width 3σ , where σ is the mass width predicted by the simulation. Over almost the entire model parameter space, σ is dominated by detector resolution. The tracker momentum scale and resolution, and the calorimeter energy scale and resolution, are tuned on the well-known $Z \rightarrow \mu\mu$ and $Z \rightarrow ee$ mass peaks [25], respectively. For $M_{\mu^*} = \Lambda$, the reconstructed $\mu\gamma$ mass resolution ranges from 9–90 GeV/c^2 for masses ranging from 200–800 GeV/c^2 .

TABLE I. Comparison of data and integrated background predictions above a given cut on the invariant mass of all $\mu\gamma$ combinations (left) and on the $\mu\mu\gamma$ invariant mass (right).

$\mu\gamma$ combinations		Events			
$m_{\mu\gamma}$ (GeV/c^2)	Data	Background	$m_{\mu\mu\gamma}$ (GeV/c^2)	Data	Background
>0	34	16.6 ± 1.8	>0	17	8.3 ± 0.9
>50	22	10.4 ± 1.1	>100	6	2.7 ± 0.3
>100	4	2.1 ± 0.3	>150	2	1.5 ± 0.2
>150	2	0.89 ± 0.14	>200	2	0.9 ± 0.1
>200	0	0.37 ± 0.07	>250	1	0.51 ± 0.09
			>300	0	0.29 ± 0.06

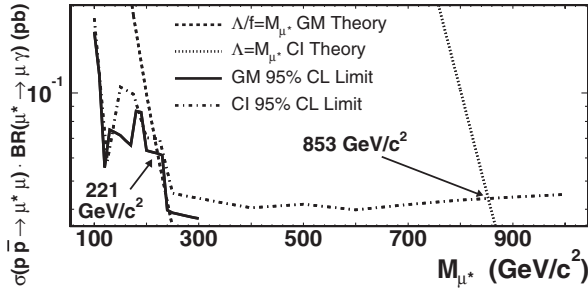


FIG. 3. The experimental cross section \times branching ratio limits at 95% CL for the CI (dashed-dotted line) and GM models (solid line), compared to the CI model prediction for $\Lambda = M_{\mu^*}$ (dotted line) and the GM model prediction for $\Lambda/f = M_{\mu^*}$ (dashed line). Also indicated are the mass values that are excluded by these data.

We use a Bayesian [26] approach, with a flat prior on the signal cross section and gamma priors on acceptance and backgrounds, to set limits on the $\mu\mu^*$ production cross section as a function of M_{μ^*} [27]. The cross section limits are converted to M_{μ^*} limits by comparing them to the next-to-next-to-leading-order (NNLO) theoretical cross sections [23], computed using the MRST set of PDFs [28]. We use the CTEQ prescription [29] to calculate the cross section uncertainty due to PDFs, which varies from 5% ($M_{\mu^*} = 100 \text{ GeV}/c^2$) to 20% ($M_{\mu^*} = 1 \text{ TeV}/c^2$). Uncertainties on higher-order QCD corrections (7%–13%) depend on M_{μ^*} and the production model.

The 95% confidence level (C.L.) upper limits on the experimental cross section \times BR are shown in Fig. 3,

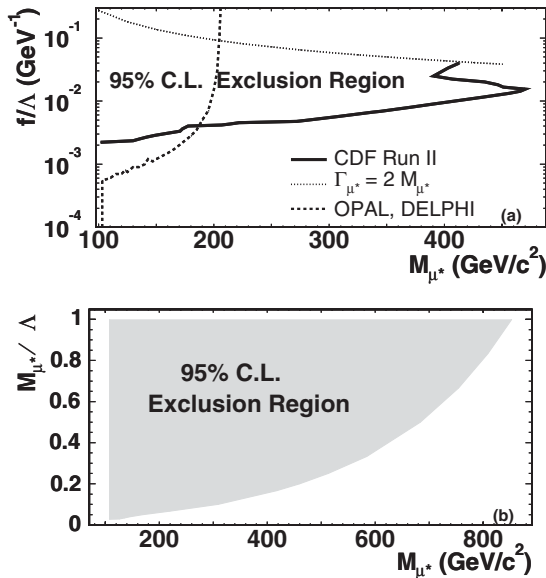


FIG. 4. The 2D parameter space regions excluded by this analysis for (a) the GM model, along with the current world limits [5], and (b) the CI model. We do not consider the region $\Gamma_{\mu^*} > 2M_{\mu^*}$ where the total width is larger than the μ^* mass.

along with the theoretical curves for $M_{\mu^*} = \Lambda/f$ ($M_{\mu^*} = \Lambda$) for the GM (CI) model. For both models, we lose sensitivity for $M_{\mu^*} < 100 \text{ GeV}/c^2$ due to large backgrounds and loss of signal acceptance. In our region of sensitivity, masses below $221 \text{ GeV}/c^2$ ($853 \text{ GeV}/c^2$) are excluded for the GM (CI) model. The CI exclusion reduces to $M_{\mu^*} < 696 \text{ GeV}/c^2$ if we use μ^* branching ratios that account for hypothetical CI decays, as assumed by the D0 collaboration [6]. Figure 4 shows the limits in the parameter space of f/Λ (M_{μ^*}/Λ) versus M_{μ^*} for the GM (CI) model. These are the world's strongest limits over much of the parameter space and complement our recent results of a search for excited and exotic electrons [4].

We are grateful to Alejandro Daleo for providing NNLO cross section calculations. We thank the Fermilab staff and the technical staffs of the participating institutions for their vital contributions. This work was supported by the U. S. Department of Energy and National Science Foundation; the Italian Istituto Nazionale di Fisica Nucleare; the Ministry of Education, Culture, Sports, Science and Technology of Japan; the Natural Sciences and Engineering Research Council of Canada; the National Science Council of the Republic of China; the Swiss National Science Foundation; the A. P. Sloan Foundation; the Bundesministerium für Bildung und Forschung, Germany; the Korean Science and Engineering Foundation and the Korean Research Foundation; the Particle Physics and Astronomy Research Council and the Royal Society, UK; the Russian Foundation for Basic Research; the Comisión Interministerial de Ciencia y Tecnología, Spain; in part by the European Community's Human Potential Programme under Contract No. HPRN-CT-2002-00292; and the Academy of Finland.

- [1] U. Baur, M. Spira, and P. M. Zerwas, Phys. Rev. D **42**, 815 (1990), and references therein.
- [2] J. L. Hewett and T. G. Rizzo, Phys. Rep. **183**, 193 (1989), and references therein.
- [3] K. Hagiwara, S. Komamiya, and D. Zeppenfeld, Z. Phys. C **29**, 115 (1985), and references therein; E. Boos *et al.*, Phys. Rev. D **66**, 013011 (2002), and references therein.
- [4] D. Acosta *et al.* (CDF Collaboration), Phys. Rev. Lett. **94**, 101802 (2005).
- [5] G. Abbiendi *et al.* (OPAL Collaboration), Phys. Lett. B **544**, 57 (2002); J. Abdallah *et al.* (DELPHI Collaboration), Eur. Phys. J. C **46**, 277 (2006).
- [6] V. Abazov *et al.* (D0 Collaboration), Phys. Rev. D **73**, 111102 (2006).
- [7] G. W. Bennett *et al.* (Muon $g - 2$ Collaboration), Phys. Rev. D **73**, 072003 (2006).
- [8] F. M. Renard, Phys. Lett. B **116**, 264 (1982).
- [9] D. Acosta *et al.* (CDF Collaboration), Phys. Rev. D **71**, 032001 (2005).
- [10] T. Affolder *et al.*, Nucl. Instrum. Methods Phys. Res., Sect. A **526**, 249 (2004).

- [11] F. Abe *et al.* (CDF Collaboration), Nucl. Instrum. Methods Phys. Res., Sect. A **271**, 387 (1988).
- [12] CDF uses a cylindrical coordinate system in which ϕ is the azimuthal angle, r is the radius from the nominal beam line, and $+z$ points in the direction of the proton beam and is zero at the center of the detector. The pseudorapidity is defined as $\eta = -\ln[\tan(\theta/2)]$, where θ is the polar angle with respect to the z axis. Calorimeter energy (track momentum) measured transverse to the beam is denoted as E_T (p_T).
- [13] M. G. Albrow *et al.*, Nucl. Instrum. Methods Phys. Res., Sect. A **480**, 524 (2002); **431**, 104 (1999); P. de Barbaro *et al.*, IEEE Trans. Nucl. Sci. **42**, 510 (1995).
- [14] G. Ascoli *et al.*, Nucl. Instrum. Methods Phys. Res., Sect. A **268**, 33 (1988).
- [15] A. Abulencia *et al.* (CDF Collaboration), hep-ex/0508029 [Phys. Rev. D (to be published)].
- [16] A. Kotwal, H. Gerberich, and C. Hays, Nucl. Instrum. Methods Phys. Res., Sect. A **506**, 110 (2003).
- [17] R. Brun and F. Carminati, CERN Program Library Long Writeup, Report No. W5013, 1993 (unpublished), version 3.15.
- [18] T. Sjöstrand, Comput. Phys. Commun. **82**, 74 (1994). We divide the μ^* production cross-section calculated by PYTHIA version 6.127 by a factor of 2, to be consistent with PYTHIA version 6.211, as described in the PYTHIA release notes.
- [19] A. V. Semenov, hep-ph/0208011; Comput. Phys. Commun. **115**, 124 (1998).
- [20] A. Pukhov *et al.*, hep-ph/9908288; E. E. Boos *et al.*, hep-ph/9503280.
- [21] U. Baur and E. L. Berger, Phys. Rev. D **47**, 4889 (1993).
- [22] S. Klimenko, J. Konigsberg, and T. M. Liss, FERMILAB, Report No. FERMILAB-FN-0741, 2003; D. Acosta *et al.*, Nucl. Instrum. Methods Phys. Res., Sect. A **494**, 57 (2002).
- [23] U. Baur, T. Han, and J. Ohnemus, Phys. Rev. D **57**, 2823 (1998); R. Hamberg, W. L. Van Neerven, and T. Matsuura, Nucl. Phys. **B359**, 343 (1991); **B644**, 403(E) (2002); R. V. Harlander and W. B. Kilgore, Phys. Rev. Lett. **88**, 201801 (2002); A. Daleo (private communication). We use NNLO cross sections evaluated with the MRST set of PDFs.
- [24] H. Gerberich, Ph.D. thesis, Duke University Institution Report No. UMI-31-78699, p. 157, 2004.
- [25] S. Eidelman *et al.* (Particle Data Group), Phys. Lett. B **592**, 1 (2004).
- [26] J. Heinrich *et al.*, physics/0409129; K. Hagiwara *et al.*, Phys. Rev. D **66**, 010001 (2002), Sec. 31.
- [27] An event is considered a μ^* candidate for a given mass hypothesis if at least one $\mu\gamma$ combination has a reconstructed mass in the sliding mass window.
- [28] A. D. Martin, R. G. Roberts, W. J. Stirling, and R. S. Thorne, Eur. Phys. J. C **4**, 463 (1998); **23**, 73 (2002).
- [29] J. Pumplin *et al.*, J. High Energy Phys. 07 (2002) 012.